Macromolecules

pubs.acs.org/Macromolecules Article

Hydroesterification of Polycyclooctene to Access Linear Ethylene Ethyl Acrylate Copolymers as a Step Toward Polyolefin Functionalization

Ikechukwu Martin Ogbu,[#] Eli J. Fastow,[#] Karen I. Winey,[*] and Marisa C. Kozlowski[*]

Cite This: https://doi.org/10.1021/acs.macromol.4c02074 Read Online

ACCESS | Metrics & More | Article Recommendations | Supporting Information

ABSTRACT: To advance a strategy of polymer-to-polymer upcycling of waste polyolefin by dehydrogenation then functionalization, we report successful hydroesterification of polycyclooctene (PCOE), an analogue for partially unsaturated polyethylene. Here, we convert PCOE to a linear analog for poly(ethylene-*co*-ethyl acrylate) (EEA) across a range of ethyl acrylate incorporations (0 to 18 mol % of ethylene units). The ester incorporation was well controlled by reaction time, and the remaining C═C bonds were subsequently hydrogenated. The bulky ethyl acrylate groups did not incorporate into orthorhombic PE crystals, decreasing the crystallinity, crystallite size, and melting temperature with increasing functionalization. Additionally, hydroesterification tuned the dynamic mechanical properties, decreasing both the glass transition temperature and the storage modulus in the rubbery regime with greater functionalization. The linear EEA analogs reported here achieve remarkable extensibility (strain > 4000%) and high toughness, comparable to commercial random and branched EEA. Ultimately, we demonstrate successful conversion of an analogue to dehydrogenated PE to a linear EEA with favorable mechanical properties.

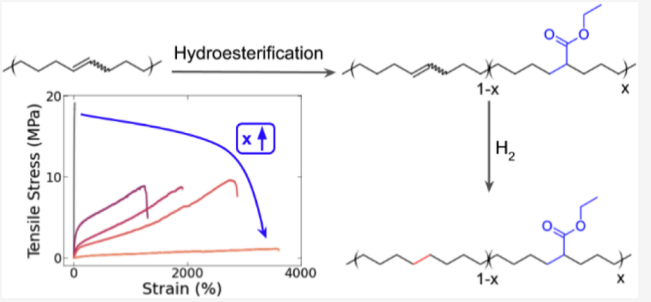

INTRODUCTION

Polyolefins constitute the majority of polymer production, primarily as single-use plastics with an average product lifetime of half a year.[1,2] The incorporation of pendant polar functionality into polyolefins produces copolymers with greater performance in applications that require high strength, toughness, and adhesion. Synthesis of polyolefin copolymers typically proceeds by free radical polymerization, producing a random distribution of functional groups and branched chain architecture.[3,4] Postpolymerization modification is, however, another strategy to incorporate functional groups on polyolefins to upgrade them to value-added functional polymers. This complementary approach also allows access to novel polymers with previously inaccessible chain architecture.[5,6] In addition, postpolymerization modification of waste polyolefins to generate functional polymers promises to recover value and keep atoms in the economy for longer. Here, we investigate the postpolymerization modification of a model for partially unsaturated polyolefin waste.[7−9]

We target the synthesis of ethylene acrylate copolymers, valued for flexibility, toughness, and adhesive properties.[20,21] They have wide applications in hot melt adhesives, sealants, plasticizers, food packaging and cable jacketing.[22−24] The market value of ethylene acrylate copolymers is increasing and expected to reach 70 billion US dollars by 2033.[25] For example, poly(ethylene-*co*-ethyl acrylate) (EEA) is typically valued for its high toughness, thermal stability, and extensibility, and is often used in cable jacketing applications.[24,26−28]

Conventionally, commercial EEA is made by copolymerization of ethylene and ethyl acrylate comonomers by a free radical process as metal-catalyzed copolymerization is challenging due to catalyst deactivation by the polar comonomers.[3,4] This free radical process leads to polymer branching. An unbranched EEA version can be prepared by ring-opening metathesis polymerization of ester-functionalized cycloalkenes or its copolymerization with other cycloakenes.[29−31] Postpolymerization modifications to incorporate pendant ester units on polyolefins through photocatalysis or free-radical C−H alkylation or using a diazo reagent have also been reported,[32,33] but the obtained polymers structurally differ from conventional ethylene acrylate copolymers in that there are additional carbon atoms between the carboxylic acid and the polymer backbone. Here, we contribute to an alternative route to EEA by hydroesterification of polycyclooctene

Received: August 30, 2024
Revised: October 21, 2024
Accepted: October 24, 2024

(PCOE), a model for partially dehydrogenated high density polyethylene (HDPE), using CO and alcohol to access linear EEA that cannot be obtained using conventional free radical methods.

Hydroesterification result in the conversion of an alkene (RCH═CHR) to a saturated unit bearing an ester ($RCH_2-CHRCO_2R'$).[34−36] This reaction has been used industrially on large scale with small molecules; for instance, ∼100 kt of methyl propionate was produced by hydroesterification of ethylene from 2000 to 2010.[34,37,38] Further, Alper and Ajjou have employed hydroesterification to functionalize more soluble and readily processable 1,2-polybutadiene.[39] This polymer contains vinyl alkene units, which react faster than internal alkenes,[40] and may not serve as a good model for partially dehydrogenated polyethylene containing predominantly internal alkenes.[19] Disubstitution of the carbon−carbon double bond exerts steric hindrance, which hampers its reactivity.[40]

We envision the hydroesterification approach reported here as part of a two-step approach to polymer-to-polymer upcycling involving partial dehydrogenation to introduce carbon−carbon double bonds and subsequent functionalization.[10−13] Upcycling of polyolefins via postpolymerization functionalization has remained a big challenge due to their chemical inertness. Although efforts have been made to directly incorporate functional groups on polyolefins using free-radical methods, this approach is often limited by poor reaction control with attendant polymer cross-linking and chain scission.[6] Other methods, such as the use of carbene-based precursors and transition metal C−H activation, often suffered from limited reactivity. Our proposed two-step approach allows easier and more controlled functionalization of polyolefins, and diverse functionalization is possible given the numerous alkene functionalizations available, as we have previously demonstrated.[10−12,14] Partial dehydrogenation of aliphatic polyolefins has been reported by Goldman and Coates groups using iridium pincer catalyst,[15−18] and has successfully been used to deconstruct polyolefins via cross-metathesis to obtain functionalized macromonomers, which could be repolymerized into higher value functional polymers.[19] Direct functionalization of partially dehydrogenated polyolefins is another strategy that can lead to functionalized polyolefins without the deconstruction of the starting polymer, thereby reducing process steps and cost.

In the present study, we functionalize PCOE, as a model for partially dehydrogenated HDPE, with ethyl acrylate units by hydroesterification. We characterize the thermal, structural, surface, and mechanical properties of this linear ethylene ethyl acrylate copolymer. Ethyl acrylate does not incorporate into crystallites, decreasing the crystallinity and melting temperature with greater functionalization. Increasing the functionalization also reduced the rubbery storage modulus and significantly increased the extensibility. Ultimately, we generate a linear equivalent of EEA and establish its mechanical properties.

■ EXPERIMENTAL DETAILS

Materials. *cis*-Cyclooctene (95%, stabilized) and *trans*-4-octene were obtained from Acros Organic. $PbCl_2(PPh_3)_2$ was purchased from Ambeed. Hoveyda−Grubbs catalyst M720 Umicore, tri-*n*-propylamine, *p*-toluenesulfonyl hydrazide, and anhydrous benzene were sourced from Sigma-Aldrich. Triphenylphosphine was purchased from Alfa Aesar. Carbon monoxide (CO, 99.99%) was obtained from Airgas company. The gas was used directly without further purification. Absolute ethanol (99.5%) and *p*-xylene were purchased from Fisher Scientific. Commercial EEA (CAS# 9010-86-0) was purchased from Scientific Polymer Products with ethyl acrylate content of 3.0 mol % as determined by high temperature ^{1}H NMR. We refer to this polymer as 3-rEEA.

Synthesis of Polycyclooctene (PCOE). *cis*-Cyclooctene (12 mL, 92 mmol) and *trans*-4-octene (0.11 mL, 0.67 mmol) were added into a two-neck round flask containing dry CH_2Cl_2 (10 mL) and magnetic stirrer. The mixture was purged with argon for 10 min. Hoveyda−Grubbs catalyst (M720) (5.8 mg) dissolved in dry CH_2Cl_2 (5 mL) under argon was added, and the reaction mixture was stirred under a positive pressure of argon for 30 min. After 5 min, the mixture became too viscous to stir and was diluted with additional CH_2Cl_2 (20 mL). The reaction was quenched by adding ethyl vinyl ether (0.5 mL). After stirring for 5 min, the product was precipitated with MeOH (400 mL) and washed with additional MeOH. The residual solvent was removed under reduced pressure overnight. The product was obtained as a white soft solid, 9.7 mg, 81%, *trans*/*cis* ratio = 1:0.23, soluble in CH_2Cl_2 at room temperature.

Functionalization of PCOE. *Hydroesterification of PCOE.* Hydroesterification was done in a well-ventilated hood using a Parr 5000 multireactor with 45 mL Hastelloy vessels equipped with Teflon liners and magnetic stirring. Note: for safety reasons, the fume hood was equipped with carbon monoxide detector (detection range: 0−1000 ppm, response time < 30s), and high-pressure regulator was used on the gas cylinder. PCOE (270 mg, 2.45 mmol C═C), $PdCl_2(PPh_3)_2$ (3 mol %, 0.0735 mmol), PPh_3 (6 mol %, 0.368 mmol), and TsOH (2 mol %, 0.049 mmol) were weighed into the liner. Absolute ethanol (4.0 mL) and dry benzene (3.0 mL) were added. The reactor was sealed and purged with argon, followed by seven cycles of CO pressure (4 atm) pressurization and depressurization. Final pressurization with CO (40 atm) was followed by heating at 140 °C for 48 h under constant stirring (1400 rpm). After it was cooled to room temperature, the reactor was depressurized, and the liquid component of the reaction mixture was decanted. The remaining soft solid was dissolved in CH_2Cl_2 (5 mL), precipitated in MeOH (50 mL), and recovered by decantation. Further purification was conducted by redissolving the polymer in CH_2Cl_2 and reprecipitation in MeOH. This process was repeated several times to obtain the functionalized polymer as a soft white solid, 320 mg.

Gelation Test. Polymer gelation was determined by dissolving the polymer (20 mg) in CH_2Cl_2 (5 mL) at room temperature for 4 h. With vacuum filtration, the undissolved polymer was separated and dried for 3 h at 50 °C under vacuum. The solid was weighed and used to determine percent gel content.

Palladium Black Removal. In some cases, palladium black was observed in the polymer, especially after a prolonged reaction time. This was removed by dissolving the polymer in excess dichloromethane (10 mL). The mixture was refrigerated overnight, during which the palladium particles sediment. The clear polymer solution was pipetted out, concentrated down to 5 mL and precipitated in MeOH. The polymer was dried at 35 °C under vacuum.

Hydrogenation of the Ethyl Acrylate Functionalized PCOE. To a two-neck round-bottom flask equipped with a reflux condenser, the functionalized polymer (300 mg), tri*n*-propylamine (5 equiv relative to residual C═C in the polymer), *p*-toluenesulfonyl hydrazide, TSH (2.5 equiv relative to the residual C═C in the polymer), and xylene (20 mL) were added. The mixture was purged with argon for 10 min and, thereafter, heated in a preheated 125 °C oil bath for 1.5 h under positive argon pressure. Another portion of TSH (2.5 equiv) was added, and the reaction continued for an additional 1.5 h. The reaction mixture was allowed to cool for about 2 min and directly precipitated in methanol while still warm. The polymer was collected by filtration, washed twice with methanol, and dried at 35 °C overnight under reduced pressure.

The functionalized and hydrogenated polymer is termed *x*-EEA, where *x* represents the fraction of ethylene units bearing ethyl acrylate functionality. We refer to this value as the functionalization, which can range from 0 to a maximum of 25% at full conversion of C═C.

https://doi.org/10.1021/acs.macromol.4c02074
Macromolecules XXXX, XXX, XXX−XXX

Table 1. Hydroesterification of PCOE Catalyzed with $PdCl_2(PPh_3)_2$ Under Different Reaction Conditions[a]

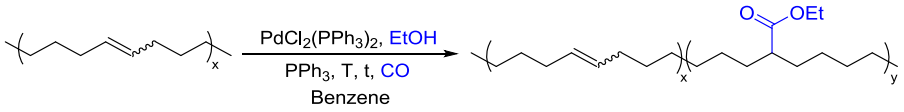

#	CO (atm)	T (°C)	t (h)	EtOH (mL)	Cosolvent	Ligand	Additive	Gelation (%)	Funct. (mol %)[b]	Funct. yield (%)[c]
1	40	140	24	4	Benzene	PPh_3	–	0	9	36
2	40	140	24	4	Benzene	PPh_3	**TsOH**	0	16	64
3	40	140	24	**7**	–	PPh_3	TsOH	0	3	12
4	**20**	140	24	4	Benzene	PPh_3	TsOH	0	13	52
5	40	**170**	24	4	Benzene	PPh_3	TsOH	0	12	48
6	40	140	24	4	Benzene	PPh_3	TsOH, **H_2** (5 atm)	0	16	64
7	40	140	24	4	Benzene	**dppb**	TsOH	>90	0.3	1.2
8	40	140	24	4	Benzene	**dtbpmb**	TsOH	>95	0.2	0.8
9	40	140	**48**	4	Benzene	PPh_3	TsOH	0	18	72
10	40	140	**72**	4	Benzene	PPh_3	TsOH	0	21	84
11	40	**100**	72	4	Benzene	PPh_3	TsOH	0	19	76
12[d]	40	140	96	4	Benzene	PPh_3	TsOH	0	16	64

[a]All reactions were performed in a Parr reactor (45 mL) using PCOE (270 mg, 2.45 mmol C═C), $PdCl_2(PPh_3)_2$ (3 mol %, 0.0735 mmol), PPh_3 (6 mol %, 0.368 mmol), TsOH (2 mol %, 0.049 mmol), ethanol (4 mL), and benzene (3 mL). dppb: 1,4-bis(diphenylphosphino)butane. dtbpmb: 1,2-bis(di-*tert*-butylphosphinomethyl) benzene. [b]Determined from ^1H NMR at 298 K, 600 MHz, using $CDCl_3$ as solvent. Maximum (all alkenes reacted) = 25 mol %. [c]Functional mol % relative to maximum (25 mol %). [d]1 g-scale.

Spectroscopic Characterization. *Nuclear Magnetic Resonance (NMR).* Room temperature NMR (^1H and ^{13}C) spectra were recorded on a Fourier transform NMR spectrometer at 298 K and 600 MHz, using $CDCl_3$ as the solvent. High temperature ^1H NMR was recorded at 363 K and 500 MHz using 1,1,2,2-tetrachloroethane-d_2 as the solvent.

Attenuated Total Reflectance (ATR)–Fourier Transform Infrared (FTIR) Spectroscopy. FTIR-ATR was taken using a Nicolet 20 FTIR with ATR attachment. Spectra were measured using an ambient temperature DTGS. Following drying at 120 °C for 4 h, polymer powder was compressed under an anvil against the diamond ATR crystal, then spectra were collected at 0.2 cm^{-1} resolution from the sum of 100 scans.

High Temperature Gel Permeation Chromatography (HT-GPC). Molecular weights and dispersities (Đ) were measured by using high temperature gel permeation chromatography with infrared detection (HT-GPC) on a Polymer Char GPC-IR instrument. This HT-GPC had a guard column, three Agilent Omniplex columns, and an IR4 detector from Polymer Char. The IR4 detector measures both total CH signal and CH_3 signal, Figure S4. All samples were dissolved in 1,2,4-trichlorobenzene at 150 °C by the instrument's autosampler with a 90 min dissolution time. Measurement proceeded at a concentration of ~1 mg/mL and molecular weights were determined against 16 narrow molecular weight polystyrene (PS) standards.

Thermal Analysis. *Thermogravimetric Analysis (TGA).* The TGA measurements were taken with a TA SDT650 scanning differential thermogravimetric analyzer. TGA measurements were conducted on ~5 mg of polymer loaded into 90 μL alumina pans at a ramp rate of 10 °C/min from 50 to 550 °C under a nitrogen atmosphere.

Differential Scanning Calorimetry (DSC). DSC measurements were conducted on dried polymer powder (~5 mg) was loaded into TZero hermetic aluminum pans. Samples were first heated to 150 °C at 20 °C/min and then held for a 5 min isotherm to erase thermal history. Samples were then cooled to −125 °C and heated to 150 °C at 10 °C/min. Heat flux data was taken from the final heating, and crystalline fraction (X_c) was determined by dividing the enthalpy of melting by 293 J/g, or the enthalpy of melting from 100% crystalline polyethylene (PE).

Film Preparation. Following drying at 120 °C for 4 h, films of *x*-EEA and 3-rEEA were prepared by loading polymer powder into window molds between two polytetrafluoroethylene (PTFE) liners and then melt pressing on a Carver hot press at 135 °C under 1.5 T of pressure. Samples were then allowed to return to room temperature on the benchtop. After melt pressing, ~5 mg of excess film was dissolved in 5 mL of tetrahydrofuran at 50 °C to confirm a lack of gelation. All *x*-EEA samples were dissolved. Melt pressed films were used for contact angle, X-ray scattering, and mechanical testing.

Contact Angle Testing. Contact angle was measured on films 1 cm in diameter prepared by the hot pressing procedure described above. Measuring the water contact angle first required applying a 10 μL droplet of water to the polymer surface and taking an image with a flat CCD camera. Contact angle was determined by fitting the drop shape to the Young–Laplace equation for an asymmetric droplet.[41]

X-Ray Scattering. Polymer films prepared by hot pressing were affixed to a standard transmission holder from Xenocs by polyimide tape. X-ray scattering was performed on a Xeuss 2.0 instrument with a Cu Kα source. Small angle X-ray scattering (SAXS) data were collected using a Pilatus 1 M solid state detector, and wide-angle X-ray scattering (WAXS) data were collected using a Dectris 100k detector. Crystallinity from X-ray scattering was determined by first fitting crystalline peaks in the WAXS signal to Lorentzian functions and the amorphous halo to a double-Gaussian function. These functions were integrated to identify I_c (total crystalline intensity) and I_a (total amorphous intensity). Crystallinity was determined by using $X_c = I_c/(I_c + I_a)$.

Mechanical Testing. *Dynamic Mechanical Analysis (DMA).* DMA measurements were conducted using a RSA III DMA from TA using 25 mm × 3 mm × 0.3 mm samples. Temperature sweep measurements proceeded at 1 Hz frequency, 0.2% strain amplitude, 10 °C/min ramp rate from −90 to 50 °C, and autotension adjustments. Autotension applied a constant strain to keep the minimum force to 20 g-equivalent and the maximum force to 300 g-equivalent in tension. Frequency/temperature sweep measurements proceeded at 0.03 to 90 Hz frequency with 10 points per decade, 0.2% strain amplitude, 10 K temperature steps from −70 to 30 °C, and autotension adjustments. Construction of the master curve was performed by identifying the horizontal shift with a custom Python script that minimized the interpolated difference between adjacent measurements normalized by the overlap window. Vertical shifts were taken from the thermal expansion of poly(ethylene-*co*-ethyl acrylate) (thermal expansion coefficient = 205 × 10^{-6} m/(m K)).[42]

Tensile Tests. Tensile tests were conducted on an Instron 5564 Tabletop Universal Testing Machine with a 2 kN load cell and pneumatic grips. Microtensile sample dimensions comply with ASTM D1708-18.[43] Five dog bone samples per polymer were strained at 1 mm/min ($d\varepsilon$ = 0.0033 s^{-1}), following the Speed B conditions in ASTM D1708-18, until failure.

https://doi.org/10.1021/acs.macromol.4c02074
Macromolecules XXXX, XXX, XXX−XXX

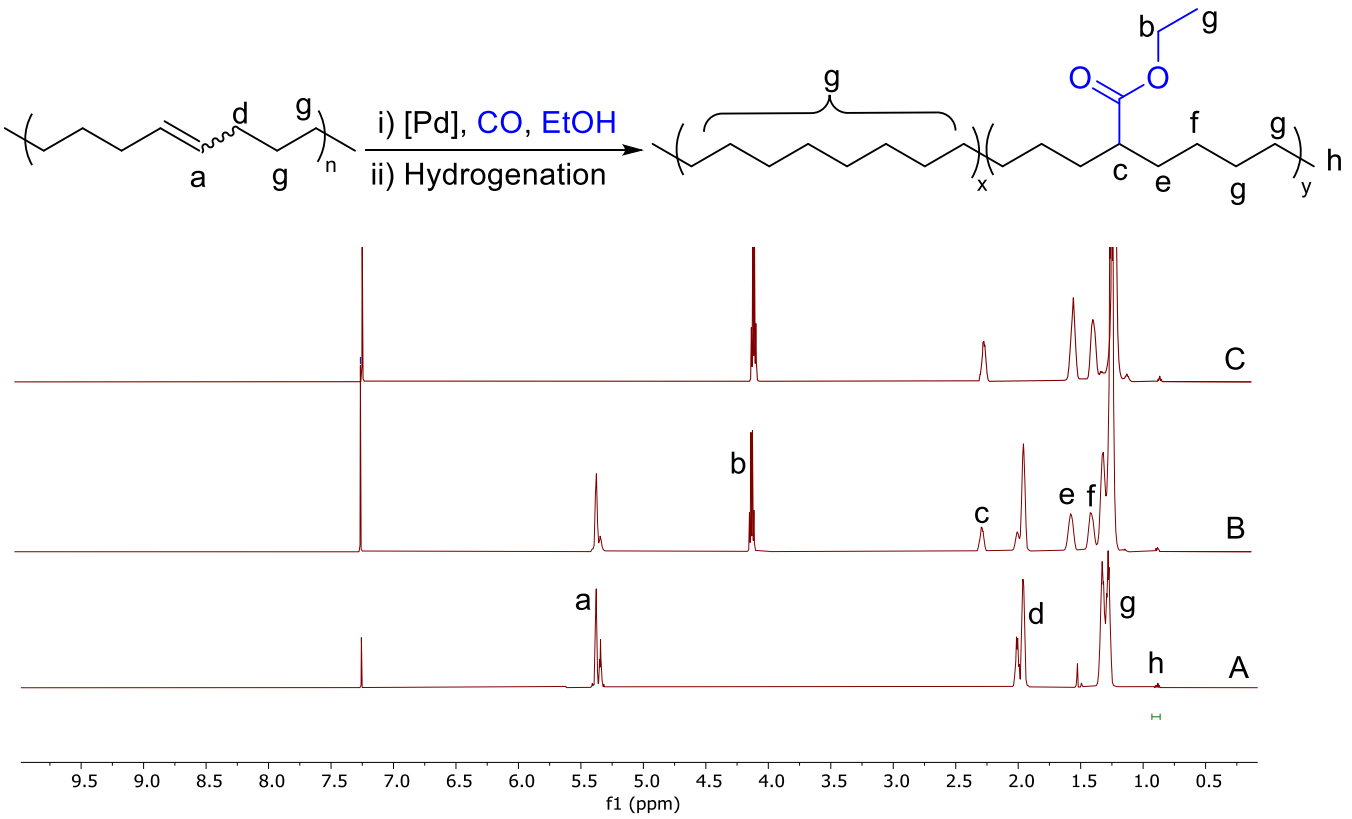

Figure 1. ^{1}H NMR of ethylene acrylate copolymers (11-EEA) before and after hydrogenation using *p*-toluenesulfonyl hydrazide, spectra recorded at 298 K, 600 MHz, using $CDCl_3$ as solvent. (A) PCOE, (B) after hydroesterification, and (C) after hydroesterification and hydrogenation.

RESULTS AND DISCUSSION

Optimization of Hydroesterification Reaction Conditions. The PCOE used as a model for partially dehydrogenated polyethylene has M_n = 12.6 kDa, M_w = 41.0 kDa, $Đ$ = 3.1, as determined by HT-GPC after hydrogenation, and *trans*/*cis* double ratio of 1/0.23 as determined by ^{1}H NMR. Based on the efficiency of palladium catalysts in the hydroesterification of small alkenes, $PdCl_2(PPh_3)_2$ was chosen as catalyst for the reaction, and PPh_3 was chosen as low-cost ligand. We targeted ethyl ester adducts to compare to commercial materials, and hence used EtOH as solvent. Benzene was selected as cosolvent to solubilize the polymers.[12] Initial trials without any additive resulted in a moderate functionalization, and no polymer gelation was observed; Table 1, entry 1. TsOH as cocatalyst provided an almost 2-fold acceleration of the reaction and also did not induce any polymer gelation, entry 2. The acid cocatalyst likely promotes the reaction by helping to generate catalytically more active palladium-hydride species, and limiting palladium black formation.[35,40] With neat ethanol, a lower ester yield was observed due to limited solubility, entry 3. Reactivity also diminished with a lower CO pressure, entry 4. Higher temperature not suitable as catalyst decomposition to Pd black and lower yield were observed, entry 5. Hydrogen as an additive[44] has no effect on the hydroesterification, entry 6. Notably, no polymer gelation was observed with PPh_3 as ligand; however, reaction with bidentate phosphines, (1,4-bis(diphenylphosphino)butane, dppb, and 1,2-bis(di*tert*-butylphosphinomethyl) benzene, dtbpmb),[45] led to significant polymer gelation, and less ester incorporation, entries 7,8. A time-dependent increase in ester incorporation was observed, which is useful for controlling the degree of functionalization, entries 2,9,10. Lower temperature provided similar yields with less catalyst decomposition, entry 11. However, the choice of higher temperature was to rule out any possible solubility limitations especially for the reaction conducted using neat ethanol (Table 1, entry 3). Finally, a 1 g-scale reaction was performed using the same amount of catalyst/ligand (0.7 mol %), resulting in a good yield by extending the reaction time to 96 h, entry 12.

The mass of EEA isolated after the hydroesterification ranged from 265−330 mg (98−79%), indicating good mass recovery. Purification after hydroesterification was done by dissolving the polymer in CH_2Cl_2 and reprecipitating in MeOH several times to obtain white material. If the resultant material was grayish, which we attribute to the presence of palladium black, it was diluted with CH_2Cl_2 and allowed to stand overnight in a refrigerator, which allowed the palladium black to sediment. The clear polymer solution was pipetted out and precipitated in MeOH to afford white polymer. Residual MeOH was finally removed under reduced pressure at 30 °C. ^{1}H NMR (Figure 1) and ^{13}C NMR (Figure S2) spectroscopy did not exhibit signals for side-products, such as polyketones,[40] and methylene proton of the ethyl ester group was clearly observed around 4.13 ppm. Notably, only one type of ester group was observed in the spectra, indicating that extensive double bond isomerization did not occur during the hydroesterification.

Hydrogenation of Functionalized PCOE. Residual double bonds in the functionalized polymers were hydrogenated using diimide generated *in situ* with *p*-toluenesulfonyl hydrazide.[46] The resultant saturated polymer was precipitated

https://doi.org/10.1021/acs.macromol.4c02074
Macromolecules XXXX, XXX, XXX−XXX

Table 2. Alkoxy Carbonylation of PCOE Catalyzed with $PdCl_2(PPh_3)_2$ at Different Reaction Conditions[a]

Sample	t (h)	Funct. (mol %)[b]	Normalized C=O peak area (arb units)[b]	Acrylate (wt %)[c]	M_n (g/mol)[d]	M_w (g/mol)[d]	$Đ$[d]
0-EEA	0	0	0.0	0	12.6	41.0	3.2
1-EEA	1	1	0.9	4	16.1	46.4	2.8
6-EEA	2	6	1.5	18	19.8	51.3	2.6
11-EEA	6	11	2.2	31	24.7	86.9	3.5
18-EEA	48	18	3.3	44	26.4	126.0	4.7

[a]All reactions were performed in a Parr reactor (45 mL) using CO (40 atm), $PdCl_2(PPh_3)$ (3 mol %), PPh_3 (15 mol %), TsOH (2 mol %), ethanol (4 mL), and benzene (3 mL) at 140 °C. [b]Calculated from C=O stretch in FTIR (~1745 cm^{-1}) normalized to the C−H symmetric stretch (~2850 cm^{-1}). [c]Determined from ^1H NMR, at 298 K, 600 MHz, using $CDCl_3$ as solvent. [d]Determined from HT-GPC at 150 °C using trichlorobenzene as the mobile phase, calibrated with polystyrene standards.

in MeOH, washed with MeOH, and residual solvent was removed under vacuum overnight at room temperature to furnish a soft white solid. Complete saturation of residual double bonds in the polymer was confirmed by ^1H NMR, as shown in Figures 1 and S3. Prior to measurement of materials properties, the polymer samples were placed under vacuum overnight at 70 °C to remove any volatile components.

Controlling Level of Functionalization. The reaction was well controlled by reaction time, allowing adjustment of ester content, Table 2. ATR-FTIR spectroscopy corroborates ^1H NMR findings of functionalization values ranging from 0 to 18 mol % of ethylene units along with complete hydrogenation, Figure S3. Specifically, the C=O stretch peak at 1745 cm^{-1} indicates the presence of ethyl acrylate, which demonstrates that the acrylate group does not participate in hydrogen bonding.[41,42] The lack of a C=C stretch at ~1640 cm^{-1} or vinyl C−H bending at ~970 cm^{-1} supports complete hydrogenation.

HT-GPC analysis of the functionalized polymers indicated little or no backbone chain scission relative to the starting PCOE, Table 2. We observe a decrease in elution time corresponding to a larger hydrodynamic radius. By calibration to 16 low dispersity polystyrene standards, we correlate the elution time to molar mass. Gradual increases in our calculated M_n and M_w with reaction time are readily attributable to both the added acrylate group and changes in configuration in solution as polarity increases with functionalization, Table 2. With only a subtle increase in dispersity and no appearance of a high molar mass shoulder, GPC indicates little or no branching or cross-linking with functionalization, Figure S4.

Thermal Stability of Functionalized Polymers. The thermal stability of the functionalized polymers was measured by TGA, as shown in Figure 2. The unfunctionalized 0-EEA sample exhibits a 5 wt % degradation temperature ($T_{d,5\ wt\ \%}$) of 455 °C. We attribute this mass loss to scission of C−C bonds. From 0 to 1.2 mol % functionalization, the $T_{d,5\ wt\ \%}$ drops to 413 °C, though further functionalization decreases the $T_{d,5\ wt\ \%}$ to a smaller extent; $T_{d,5\ wt\ \%}$ for 18-EEA is 394 °C, Figure 2b. Prior investigations into EEA ranging from 7.9 to 28.6 mol % also identify a subtle decrease (~10 °C) in $T_{d,5\ wt\ \%}$ with greater functionalization.[47] This mass loss likely stems from decarboxylation and alcohol production mechanisms previously reported for ethyl acrylate pendant groups.[23,48]

Notably, the linear x-EEA reported here exhibits a slightly higher $T_{d,5\ wt\ \%}$ than 3-rEEA, indicating favorable thermal stability when compared to commercial equivalents. Ultimately, TGA reveals that x-EEA exhibits sufficient thermal stability for melt processing, Figure 2.

Morphology. DSC reveals a substantial monotonic decrease in melting temperature and melting enthalpy with

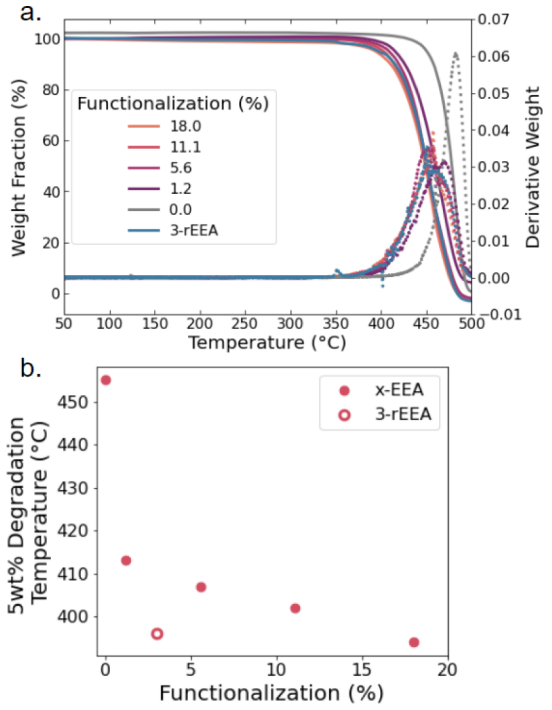

Figure 2. (a) TGA at 10 °C/min ramp rate of x-EEA (purple to orange) and 3-rEEA (blue) with weight fraction represented in solid lines and derivative weight fraction shown in dashed lines; (b) temperature corresponding to 5% weight loss plotted against functionalization from ^1H NMR.

greater functionalization, Figure 3. Notably, 1-EEA exhibits two melting exothermic peaks, a sharp peak at higher temperatures and a broad peak at lower temperatures. All of the other x-EEA polymers (except 18-EEA) exhibit a single melting feature. Commercial 3-rEEA exhibits greater T_m than the lower melting feature of 1-EEA and 6-EEA by >25 °C, Figure 3b.

X-ray scattering detects crystalline peaks at lower functionalization levels and an amorphous halo at wide angles (q > 1.0 $Å^{-1}$). WAXS clearly reveals that all samples with detectable crystalline peaks take an orthorhombic crystal structure with lattice parameters a = 7.4 Å and b = 5.0 Å, similar to HDPE.[49] The large ethyl acrylate pendants are not expected to incorporate into the crystallites,[50,51] consistent with the WAXS peak positions changing by <0.02 $Å^{-1}$ with functionalization, Figure 4a. This orthorhombic crystal structure allows us to use the enthalpy of melting corresponding to 100% crystalline PE (293 J/g) to identify the crystallinity from the heat flux in DSC, Figure 4b. DSC and X-ray scattering results are in good agreement and detect a decrease in crystallinity

https://doi.org/10.1021/acs.macromol.4c02074
Macromolecules XXXX, XXX, XXX−XXX

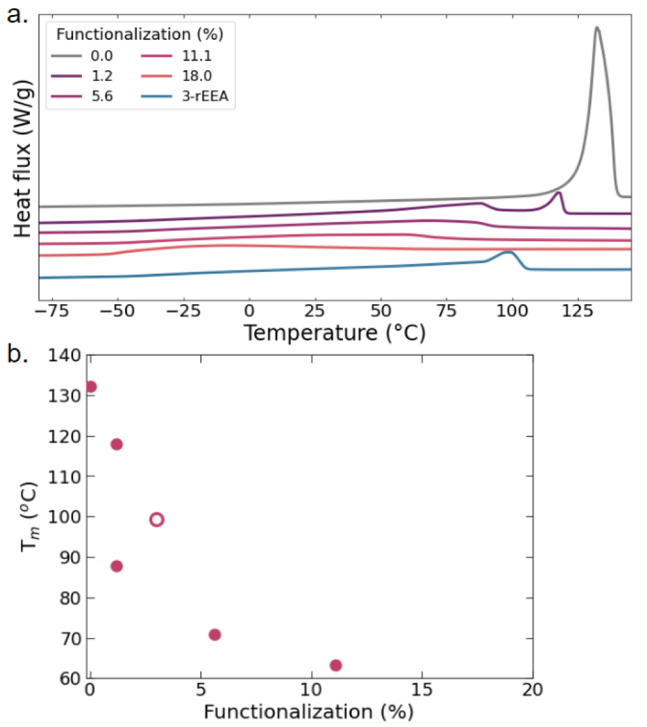

Figure 3. (a) Heat flux measured on second heating cycle (at 10 °C/min) following a 5 min isothermal hold at 150 °C and cool at 10 °C/min to −125 °C to erase thermal history and (b) melting temperature as a function of functionalization (filled circles represent *x*-EEA and open circles represent 3-rEEA).

from ∼60% in the unfunctionalized polymer to 0% at 18% functionalization. A similar decrease in crystallinity with functionalization levels, was also observed when PCOE was functionalized with thio-ether pendants.[10,11]

Crystallite size was approximated using Scherrer analysis of the full width half-maximum value extracted from the Lorentzian fit of the (110) orthorhombic peak.[52] With increasing functionalization, we observe a decrease in crystallite width from ∼850 to 200 Å, Figure 4c, that is consistent with the drop in percent crystallinity and melting temperature, Figure 3b. Additionally, the exclusion of functional groups from crystallites decreases the melt entropy, contributing to the decrease in melting temperature.[50]

Finally, we attribute the difference in melting temperature and crystallinity between *x*-EEA and 3-rEEA to the difference in the pendant arrangement along the backbone. Unlike the *x*-EEA reported here, 3-rEEA contains ethyl acrylates randomly distributed along the backbone with a minimum separation of 1 backbone carbon.[53,54] Thus, at similar compositions, 3-rEEA has some longer runs of PE that enable the formation of larger crystals that melt at higher temperatures.[50,55] Specifically, 3-rEEA exhibits a crystallite width ∼30% larger than expected for *x*-EEA at the same composition, Figure 4c, which is consistent with the higher T_m found in 3-rEEA.

Surface Polarity Increases with Functionalization. From 0 to 18 mol % functionalization contact angle decreases from 93.0 ± 1.4° to 72.9 ± 0.9°, indicating a more polar surface, Figure 5. This matches expectations as acrylate groups are more polar than the unfunctionalized ethylene monomeric units and the large ethyl acrylate pendants are expelled from the crystals and disproportionately reside in the amorphous phase expected at the surface.[12,50] The linear *x*-EEA polymers reported in this paper exhibit surface polarities similar to those of commercial EEA at comparable ethyl acrylate incorporation.

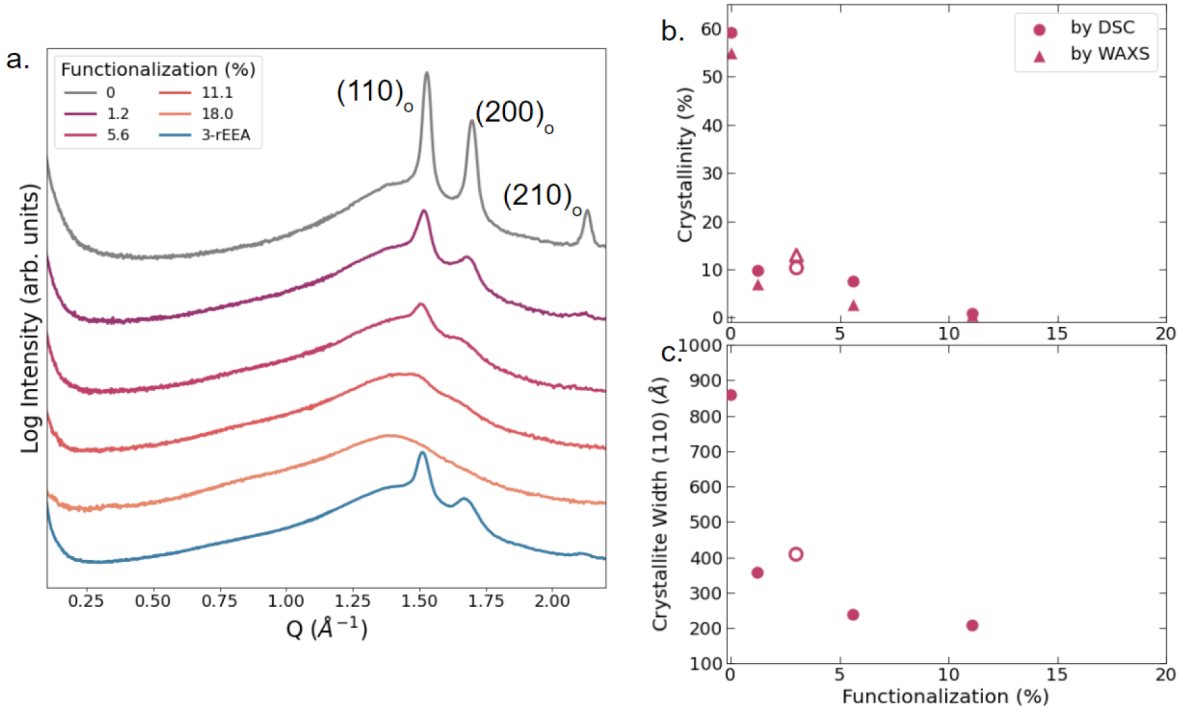

Figure 4. (a) X-ray scattering of *x*-EEA and 3-rEEA. We attribute the peaks at wide angles (>1 Å^{-1}) to crystalline scattering from an orthorhombic lattice and fit them to Lorentzian functions to calculate (b) crystallinity along with (c) crystallite width as a function of functionalization. Crystallinity was also identified by dividing the enthalpy of melting measured in DSC by 293 J/g, the reference enthalpy for 100% crystalline PE. Filled symbols correspond to *x*-EEA and empty symbols correspond to 3-rEEA.

https://doi.org/10.1021/acs.macromol.4c02074
Macromolecules XXXX, XXX, XXX−XXX

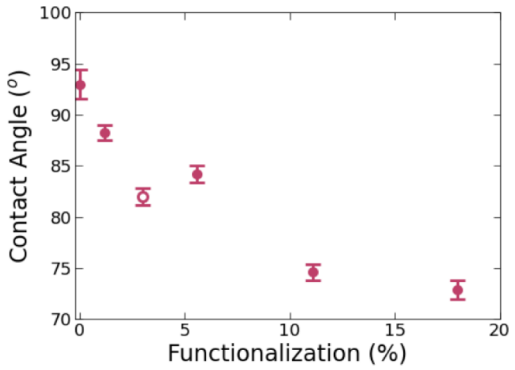

Figure 5. Contact angle of *x*-EEA (solid circles) and 3-rEEA (open circle) plotted against functionalization from ^{1}H NMR.

Thus, the linear polymers reported here may offer similar adhesion properties to commercial material; a favorable characteristic in a material often used in multilayer cable jackets or laminates.[24,28]

Tensile and Dynamic Mechanical Properties. Functionalizing PCOE with ethyl acrylate tunes the dynamic mechanical properties, as investigated by DMA, as shown in Figure 6. The measured temperature range (−90 to 50 °C) captures the glassy plateau, glass transition, rubbery plateau, and the start of the terminal relaxation, allowing us to determine the T_g and plateau moduli.[56] Glassy and rubbery plateaus were determined from E' values 30 K above and below the T_g identified from the peak in the tan(δ) curve. The glassy moduli of *x*-EEA are comparable to that of 3-rEEA, and are independent of the functionalization level. This result demonstrates that the ethyl acrylate concentration does not significantly influence glassy response.[57] This matches our prior observations of the glassy modulus of PCOE functionalized with thioether methylene carboxylic acid pendants as well as previous measurements of EEA.[11,51] However, the rubbery modulus decreases by nearly 3 orders of magnitude over the functionalization range explored, Figure 6c. From 0-EEA to 1-EEA, the rubbery modulus drops by over an order of magnitude. We attribute this significant decrease to the 6-fold loss of crystallinity between the two samples ($X_c \sim 60$ to 10%), wherein the crystalline phase stiffens the polymers in the rubbery state.

Glass transition temperatures of *x*-EEA polymers are < −30 °C, with a ∼18 °C decrease in T_g from 1 to 18% functionalization, Figure 7. These acrylate pendants act as short chain branches, and an increase in branching is well-known to increase polymer mobility and corresponding decrease in T_g.[58] The time scales corresponding to the segmental relaxation, as determined from loss modulus in frequency−temperature sweeps in DMA, confirm this increase in polymer mobility, Figure S12. Prior studies of polyolefins with short-chain branching reveal a decrease in T_g with greater short-chain branching with the T_g of a model short-chain

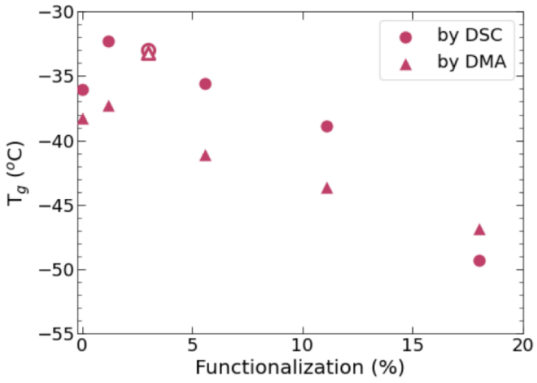

Figure 7. Glass transition temperature from both DSC and the peak of tan(δ) in DMA of *x*-EEA (solid circles) and 3-rEEA (open circle) plotted against functionalization from ^{1}H NMR.

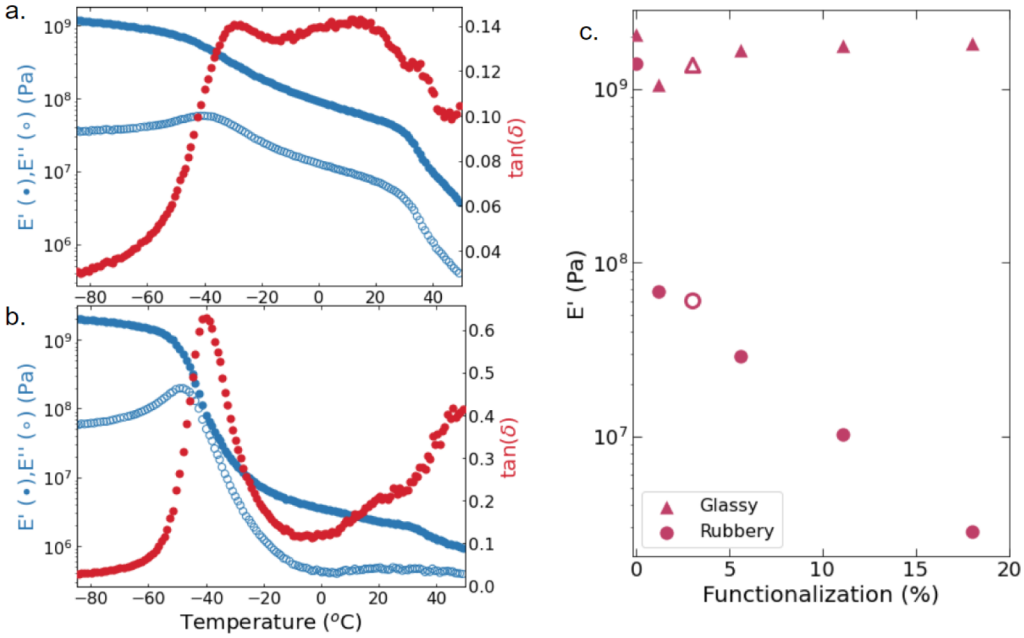

Figure 6. Temperature sweep DMA (1 Hz oscillation at a 10 °C/min ramp rate) of (a) 1-EEA and (b) 18-EEA. (c) Glassy and rubbery plateau moduli taken from the E' at $T_g \pm 30$ K.

https://doi.org/10.1021/acs.macromol.4c02074
Macromolecules XXXX, XXX, XXX−XXX

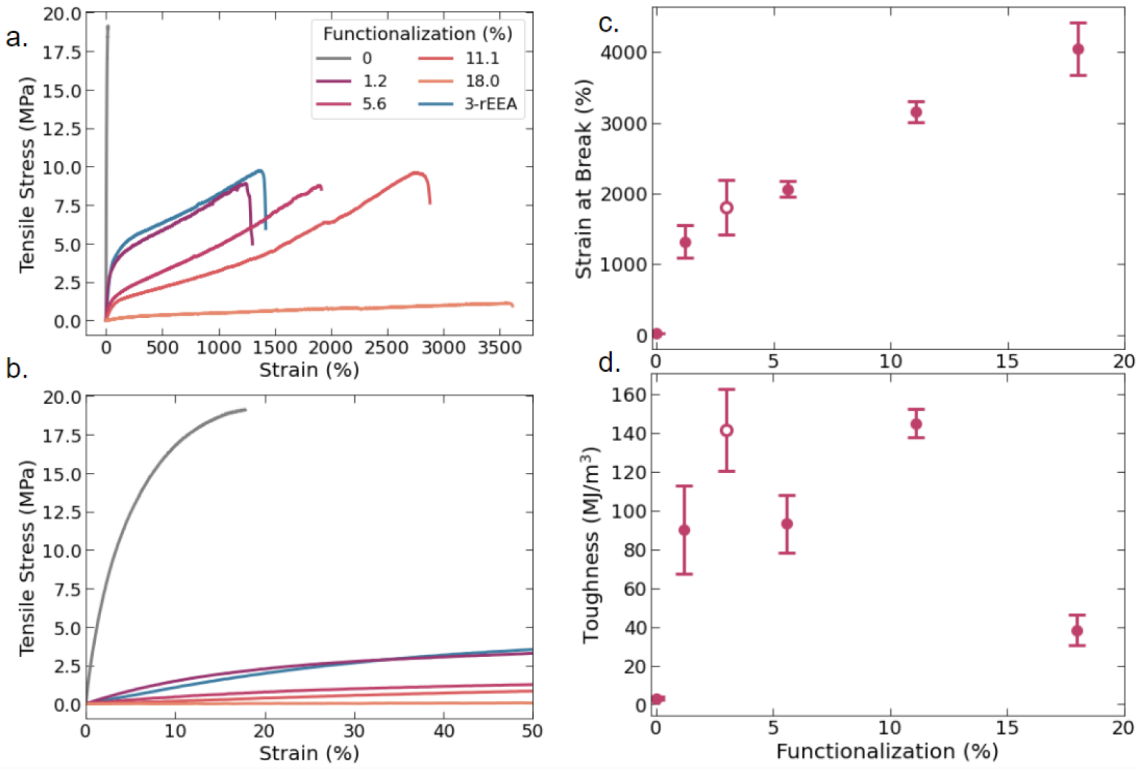

Figure 8. Representative stress−strain curves of *x*-EEA and 3-rEEA (a) until failure and (b) focused on the low strain regime. (c) Strain at break and (d) toughness were taken from the average of five measurements with error bars from the standard deviation.

Table 3. Characteristic tensile properties of *x*-EEA along with functionalization and crystallinity calculated from the heat flux in DSC[a]

	X_c (%)	*YS* (MPa)	*E* (MPa)	*UTS* (MPa)	ε at break (%)	Toughness (MJ/m^3)
0-EEA	59.2	14.0 ± 0.9	265.9 ± 7.7	20.0 ± 0.9	20.2 ± 4.9	3.04 ± 0.8
1-EEA	9.9	2.3 ± 0.1	17.8 ± 1.1	8.3 ± 1.7	1320 ± 233	90 ± 22.8
6-EEA	7.5	0.9 ± 0.6	3.4 ± 0.9	8.0 ± 1.4	2060 ± 110	93 ± 14.8
11-EEA	0.9	0.9 ± 0.7	1.2 ± 0.5	9.4 ± 0.3	3160 ± 149	145 ± 7.3
18-EEA	0	0.2 ± 0.1	0.2 ± 0.1	1.9 ± 0.4	4050 ± 374	38 ± 7.8
3-rEEA	10.4	2.1 ± 1.2	6.6 ± 3.5	11.5 ± 1.4	1800 ± 381	141 ± 41.0

[a]X_c represents % crystallinity, *YS* represents yield strength, *E* represents Young's modulus, and *UTS* represents ultimate tensile strength.

branched polyethylene decreasing by ∼20 °C from 1 to 10 mol % 1-hexene comonomer.[58−60]

Consistent with previous measurements of HDPE, the 0-EEA sample exhibited an elastic modulus of 265.9 ± 7.6 MPa and yield stress of 14.0 ± 0.6 MPa, Figure 8a,b.[61,62] The 0-EEA exhibits a lower elongation than other HDPE samples, readily attributable to the lower molecular weight in 0-EEA compared to HDPE in prior measurements.[61] As functionalization increases, the room temperature extensibility increases significantly, from a strain at break of 1320 ± 233% to 4050 ± 375% from 1-EEA to 18-EEA, Figure 8c. This 3-fold increase in extensibility corresponds with a notable decrease in elastic modulus (*E*) and yield stress (*YS*), Table 3.

From DMA, we observe a decrease in rubbery plateau modulus with increasing functionalization, Figure 6, indicating decreasing entanglement density in the amorphous that facilitates greater extension.[63−66] Additionally, the fraction of the soft amorphous domain increases with functionalization. Thus, the high significant extensibility of linear *x*-EEA is expected and is in line with the result from 3-rEEA.

These new *x*-EEA polymers add to the cannon of the polyolefin elastomer literature. Adding short-chain branching to polyethylene by copolymerization, usually with an *n*-alkene comonomer or with an acrylate, is a well-established strategy to generate polyolefin elastomers and is understood to increase ductility while decreasing *E* and *YS* as comonomer content increases.[67−69] For example, poly(ethylene-*co*-octene) polymers with comparable molecular weights and comonomer fractions to our *x*-EEA polymer exhibit three times less extensibility than reported here.[70] The significant decrease in the rubbery plateau modulus with functionalization observed in *x*-EEA and the corresponding decrease in entanglement density contribute to the high extensibility of these new polyolefin elastomers.

From 0-EEA to 11-EEA, the toughness increases significantly, from 3 ± 0.8 to 145 ± 7.3 MJ/m^3, respectively, Figure 8d. This increase in toughness is largely attributed to the increase in extensibility and the stabilizing role of crystalline domains. As expected, the completely amorphous 18-EEA sample exhibits a lower toughness than any other functionalized sample.

https://doi.org/10.1021/acs.macromol.4c02074
Macromolecules XXXX, XXX, XXX−XXX

CONCLUSION

Hydroesterification followed by hydrogenation of PCOE successfully generates linear analogs of ethylene/ethyl acrylate copolymers. Spectroscopic analysis indicated clean conversion with no observed side product formation. Moreover, we did not observe significant chain scission or cross-linking as a consequence of functionalization, and the resulting *x*-EEA was easily purified.

All *x*-EEA samples exhibited favorable thermal stability, comparable to that of commercial 3-rEEA. The bulky ethyl acrylate pendant groups disrupt PE orthorhombic crystallization, decreasing crystallite size, crystallinity, and T_m. Increasing functionalization significantly decreases the rubbery plateau storage modulus and increases extensibility. Toughness increases from 0 to 11% functionalization and compares favorably to commercial 3-rEEA.

In summary, we report a pathway to generate thermoplastics with remarkable extensibility and toughness from an analog of partially dehydrogenated HDPE. Notably, current polyethylene dehydrogenation strategies achieve ∼1% alkene bonds.[13,15−17] Fully converting these alkene bonds to ethyl acrylate groups using the chemistry described here would result in polymers comparable to 1-EEA, which exhibits mechanical properties similar to 3-rEEA. These results suggest a linear EAA prepared by dehydrogenation followed by functionalization exhibits sufficient properties for applications. Further studies would include development of a more stable ligand for the reaction, especially one that could permit catalyst recyclability,[71] thereby improving the viability of the method for polymer functionalization.

ASSOCIATED CONTENT

Supporting Information

The Supporting Information is available free of charge at https://pubs.acs.org/doi/10.1021/acs.macromol.4c02074.

Supporting Information contains additional experimental details along with additional results from ^{13}C NMR, ^{1}H NMR, FTIR, GPC, DMA, and tensile tests (PDF)

AUTHOR INFORMATION

Corresponding Authors

Karen I. Winey − *Department of Materials Science and Engineering, University of Pennsylvania, Philadelphia, Pennsylvania 19104, United States; Department of Chemical and Biomolecular Engineering, University of Pennsylvania, Philadelphia, Pennsylvania 19104, United States;* orcid.org/0000-0001-5856-3410; Email: winey@seas.upenn.edu

Marisa C. Kozlowski − *Department of Chemistry, University of Pennsylvania, Philadelphia, Pennsylvania 19104, United States;* orcid.org/0000-0002-4225-7125; Email: marisa@sas.upenn.edu

Authors

Ikechukwu Martin Ogbu − *Department of Chemistry, University of Pennsylvania, Philadelphia, Pennsylvania 19104, United States;* orcid.org/0000-0002-9053-7519

Eli J. Fastow − *Department of Materials Science and Engineering, University of Pennsylvania, Philadelphia, Pennsylvania 19104, United States;* orcid.org/0000-0003-2674-2056

Complete contact information is available at: https://pubs.acs.org/10.1021/acs.macromol.4c02074

Author Contributions

#Co-first A.M.O. conducted data curation, formal analysis, investigation, methodology, visualization, writing of original draft, and review and editing. E.F. perfoemed data curation, formal analysis, investigation, methodology, visualization, writing of original draft, and review and editing. K.I.W. worked on conceptualization, funding acquisition, project administration, supervision, review and editing of the manuscript. M.C.K. carried out conceptualization, funding acquisition, supervision, review and editing of the manuscript. ‡These authors contributed equally.

Notes

The authors declare no competing financial interest.

ACKNOWLEDGMENTS

The authors gratefully acknowledge funding by DOE BES (DESC0022238). The authors also wish to acknowledge Prof. Russel Composto (Univ. Pennsylvania) for the use of his contact angle measurement system and Steve Szewczyk (Univ. Pennsylvania) for his assistance with the DSC, DMA, and tensile testing instruments. The authors thank Roshni J. Chethalen and Prof. E. Bryan Coughlin (Univ. Massachusetts, Amherst) for assistance and helpful discussions. Partial NMR instrumentation support was provided by the NIH (3R01GM118510-03S1, 3R01GM087605-06S1) and Vagelos Institute for Energy Science and Technology. E.J.F. and K.I.W. acknowledge the use of the Dual Source and Environmental X-ray Scattering facility operated by the Laboratory for Research on the Structure of Matter at the University of Pennsylvania supported by NSF through DMR-2309043 grant.

REFERENCES

(1) Vogt, B. D.; Stokes, K. K.; Kumar, S. K. Why Is Recycling of Postconsumer Plastics so Challenging? *ACS Appl. Polym. Mater.* **2021**, *3* (9), 4325−4346.

(2) *New Plastics Economy: Rethinking the future of plastics*. https://www.ellenmacarthurfoundation.org/the-new-plastics-economy-rethinking-the-future-of-plastics. (Accessed July 7, 2024).

(3) D'Auria, I.; Saki, Z.; Liu, M.; Sun, W.-H.; Pellecchia, C. Copolymerization of Ethylene and Methyl Acrylate by Dibenzocycloheptyl-Substituted Aryliminopyridyl Ni(II) Catalysts. *Macromol* **2022**, *2* (4), 500−508.

(4) Xiong, S.; Shoshani, M. M.; Zhang, X.; Spinney, H. A.; Nett, A. J.; Henderson, B. S.; Miller, T. F.; Agapie, T. Efficient Copolymerization of Acrylate and Ethylene with Neutral P, O-Chelated Nickel Catalysts: Mechanistic Investigations of Monomer Insertion and Chelate Formation. *J. Am. Chem. Soc.* **2021**, *143* (17), 6516−6527.

(5) Neidhart, E. K.; Hua, M.; Peng, Z.; Kearney, L. T.; Bhat, V.; Vashahi, F.; Alexanian, E. J.; Sheiko, S. S.; Wang, C.; Helms, B. A.; Leibfarth, F. A. C−H Functionalization of Polyolefins to Access Reprocessable Polyolefin Thermosets. *J. Am. Chem. Soc.* **2023**, *145* (50), 27450−27458.

(6) Williamson, J. B.; Lewis, S. E.; Johnson, R. R.; Manning, I. M.; Leibfarth, F. A. C−H Functionalization of Commodity Polymers. *Angew. Chem. Int. Ed.* **2019**, *58* (26), 8654−8668.

(7) Matthews, M.; Van Reenen, A. Recycling of Polyolefins for Multiple Lifecycles. *Macromol. Mater. Eng.* **2024**, *309*, 2300421.

(8) Goring, P. D.; Priestley, R. D. Polymer Recycling and Upcycling: Recent Developments toward a Circular Economy. *JACS Au* **2023**, *3* (10), 2609−2611.

(9) Cen, Z.; Han, X.; Lin, L.; Yang, S.; Han, W.; Wen, W.; Yuan, W.; Dong, M.; Ma, Z.; Li, F.; Ke, Y.; Dong, J.; Zhang, J.; Liu, S.; Li, J.; Li, Q.; Wu, N.; Xiang, J.; Wu, H.; Cai, L.; Hou, Y.; Cheng, Y.; Daemen,

L. L.; Ramirez-Cuesta, A. J.; Ferrer, P.; Grinter, D. C.; Held, G.; Liu, Y.; Han, B. Upcycling of Polyethylene to Gasoline through a Self-Supplied Hydrogen Strategy in a Layered Self-Pillared Zeolite. *Nat. Chem.* **2024**, *16*, 871.

(10) Chethalen, R. J.; Fastow, E. J.; Coughlin, E. B.; Winey, K. I. Thiol−Ene Click Chemistry Incorporates Hydroxyl Functionality on Polycyclooctene to Tune Properties. *ACS Macro Lett.* **2023**, *12* (1), 107−112.

(11) Fastow, E.; Chethalen, R. J.; Coughlin, E. B.; Winey, K. I. Thiol-Ene Click Chemistry Incorporates Carboxylic Acid-Terminated Alkane Pendants on Polycyclooctene to Tune Properties. *Giant* **2024**, *17*, 100231.

(12) Ogbu, I. M.; Fastow, E. J.; Zhu, W.; Wells, L. A.; Chethalen, R. J.; Nair, V.; Hinton, Z. R.; Balzer, A. H.; Hu, W.; Coughlin, E. B.; Winey, K. I.; Kozlowski, M. C. Hydrocarboxylation of C═C Bonds in Polycyclooctene: Progress Toward Valorization of Waste Polyolefins. *Macromolecules* **2024**, *57* (12), 5860−5869.

(13) Hunt, S. B.; Delferro, M. Dehydrogenated Polyethylene from Discarded Plastics as a Synthon for Functional Polyolefins. *ACS Appl. Polym. Mater.* **2024**, *6* (15), 8727−8732.

(14) Ogbu, I. M.; Tu, C.-H.; Fastow, E.; Hinton, Z. R.; Winey, K. I.; Kozlowski, M. C. N_2O Deconstruction of Polycyclooctene to Generate Carbonyl-Functionalized Macromonomers. *Polym. Degrad. Stab.* **2024**, *229*, 110987.

(15) Ray, A.; Zhu, K.; Kissin, Y. V.; Cherian, A. E.; Coates, G. W.; Goldman, A. S. Dehydrogenation of Aliphatic Polyolefins Catalyzed by Pincer-Ligated Iridium Complexes. *Chem. Commun.* **2005**, *27*, 3388−3390.

(16) Ellis, L. D.; Orski, S. V.; Kenlaw, G. A.; Norman, A. G.; Beers, K. L.; Román-Leshkov, Y.; Beckham, G. T. Tandem Heterogeneous Catalysis for Polyethylene Depolymerization via an Olefin-Intermediate Process. *ACS Sustainable Chem. Eng.* **2021**, *9* (2), 623−628.

(17) Ray, A.; Kissin, Y. V.; Zhu, K.; Goldman, A. S.; Cherian, A. E.; Coates, G. W. Catalytic Post-Modification of Alkene Polymers. *J. Mol. Catal. A: Chem.* **2006**, *256* (1−2), 200−207.

(18) Zhu, K.; Achord, P. D.; Zhang, X.; Krogh-Jespersen, K.; Goldman, A. S. Highly Effective Pincer-Ligated Iridium Catalysts for Alkane Dehydrogenation. DFT Calculations of Relevant Thermodynamic, Kinetic, and Spectroscopic Properties. *J. Am. Chem. Soc.* **2004**, *126* (40), 13044−13053.

(19) Arroyave, A.; Cui, S.; Lopez, J. C.; Kocen, A. L.; LaPointe, A. M.; Delferro, M.; Coates, G. W. Catalytic Chemical Recycling of Post-Consumer Polyethylene. *J. Am. Chem. Soc.* **2022**, *144* (51), 23280−23285.

(20) *ELVALOY™ AC 2103 Acrylate Copolymer*. https://www.dow.com/en-us/pdp.elvaloy-ac-2103-acrylate-copolymer.503551z.html. (Accessed December 9, 2023).

(21) Peykova, Y.; Lebedeva, O. V.; Diethert, A.; Müller-Buschbaum, P.; Willenbacher, N. Adhesive Properties of Acrylate Copolymers: Effect of the Nature of the Substrate and Copolymer Functionality. *Int. J. Adhes. Adhes.* **2012**, *34*, 107−116.

(22) Pereira, G. G.; Figueiredo, S.; Fernandes, A. I.; Pinto, J. F. Polymer Selection for Hot-Melt Extrusion Coupled to Fused Deposition Modelling in Pharmaceutics. *Pharmaceutics* **2020**, *12* (9), 795.

(23) Wargotz, B. Thermal-oxidative Behavior of Ethylene Alkyl Acrylate Copolymers. *Polym. Eng. Sci.* **1968**, *8* (1), 50−57.

(24) Halle, R. W. New Ethylene-Methyl Acrylate Copolymers for Multilayer Flexible Packaging Applications. *J. Plast. Film Sheeting* **1989**, *5* (1), 56−65.

(25) Ethylene Copolymers Market Size, Share | CAGR of 3.7%: Market.us. https://market.us/report/ethylene-copolymers-market/. (Accessed July 14, 2024).

(26) Geussens, T. Thermoplastics for Cables. *The Global Cable Industry*; Beyer, G., Eds.; Wiley, 2021; pp 21−55. .

(27) Mildner, R. A Review of Resistive Compounds for Primary URD Cables. *IEEE Trans. Power Appar. Syst.* **1970**, *PAS-89* (2), 313−318.

(28) Moyano, M. A.; París, R.; Martín-Martínez, J. M. Viscoelastic and Adhesion Properties of Hot-Melts Made with Blends of Ethylene-Co-n-Butyl Acrylate (EBA) and Ethylene-Co-Vinyl Acetate (EVA) Copolymers. *Int. J. Adhes. Adhes.* **2019**, *88*, 34−42.

(29) Song, S.; Xing, Z.; Cheng, Z.; Fu, Z.; Xu, J.; Fan, Z. Functional Polyethylene with Regularly Distributed Ester Pendants via Ring-Opening Metathesis Polymerization of Ester Functionalized Cyclopentene: Synthesis and Characterization. *Polymer* **2017**, *129*, 135−143.

(30) Lena, J.-B.; Jackson, A. W.; Chennamaneni, L. R.; Wong, C. T.; Lim, F.; Andriani, Y.; Thoniyot, P.; Van Herk, A. M. Degradable Poly(Alkyl Acrylates) with Uniform Insertion of Ester Bonds, Comparing Batch and Semibatch Copolymerizations. *Macromolecules* **2020**, *53* (10), 3994−4011.

(31) Zhong, H.; Zhou, F.; Zhang, F.; Xu, J.; Peng, D.; He, X. Original Synthesis of Ethylene-Acrylic Acid (Ester) Copolymers Derivatives from 5-substituted Cyclooctenes with A Controllable Way Via Ring-Opening Metathesis Polymerization. *Macromol. Chem. Phys.* **2024**, *225* (2), 2300171.

(32) Zhang, Z.; Zhang, Y.; Zeng, R. Photoinduced Iron-Catalyzed C−H Alkylation of Polyolefins. *Chem. Sci.* **2023**, *14* (35), 9374−9379.

(33) Díaz-Requejo, M. M.; Wehrmann, P.; Leatherman, M. D.; Trofimenko, S.; Mecking, S.; Brookhart, M.; Pérez, P. J. Controlled, Copper-Catalyzed Functionalization of Polyolefins. *Macromolecules* **2005**, *38* (12), 4966−4969.

(34) Clegg, W.; Elsegood, M. R. J.; Eastham, G. R.; Tooze, R. P.; Wang, X. L.; Whiston, K. Highly Active and Selective Catalysts for the Production of Methyl Propanoate via the Methoxycarbonylation of Ethene. *Chem. Commun.* **1999**, *18*, 1877−1878.

(35) Jameel, F.; Kohls, E.; Stein, M. Mechanism and Control of the Palladium-Catalyzed Alkoxycarbonylation of Oleochemicals from Sustainable Sources. *ChemCatchem* **2019**, *11* (19), 4894−4906.

(36) Del Río, I.; Claver, C.; van Leeuwen, P. W. N. M. On the Mechanism of the Hydroxycarbonylation of Styrene with Palladium Systems. *Eur. J. Inorg. Chem.* **2001**, *2001* (11), 2719−2738.

(37) Yang, J.; Liu, J.; Ge, Y.; Huang, W.; Ferretti, F.; Neumann, H.; Jiao, H.; Franke, R.; Jackstell, R.; Beller, M. Efficient Palladium-Catalyzed Carbonylation of 1,3-Dienes: Selective Synthesis of Adipates and Other Aliphatic Diesters. *Angew. Chem. Int. Ed.* **2021**, *60* (17), 9527−9533.

(38) Dong, K.; Fang, X.; Gülak, S.; Franke, R.; Spannenberg, A.; Neumann, H.; Jackstell, R.; Beller, M. Highly Active and Efficient Catalysts for Alkoxycarbonylation of Alkenes. *Nat. Commun.* **2017**, *8* (1), 14117.

(39) Ajjou, A. N.; Alper, H. Catalytic Hydrocarboxylation and Hydroesterification Reactions of 1,2-Polybutadiene. *Macromolecules* **1996**, *29* (5), 1784−1788.

(40) Kiss, G. Palladium-Catalyzed Reppe Carbonylation. *Chem. Rev.* **2001**, *101* (11), 3435−3456.

(41) Stalder, A. F.; Melchior, T.; Müller, M.; Sage, D.; Blu, T.; Unser, M. Low-Bond Axisymmetric Drop Shape Analysis for Surface Tension and Contact Angle Measurements of Sessile Drops. *Colloids Surf., A* **2010**, *364* (1−3), 72−81.

(42) Wypych, G. *Handbook of Polymers*; Elsevier, 2016.

(43) D20 Committee. *Standard Test Method for Determining Molecular Weight Distribution and Molecular Weight Averages of Polyolefins by High Temperature Gel Permeation Chromatography*: ASTM International..

(44) Cavinato, G.; Toniolo, L.; Botteghi, C.; Gladiali, S. Hydrocarbo Alkoxylation of N-Vinylphthalimide Catalyzed by Palladium Complexes. *J. Organomet. Chem.* **1982**, *229* (1), 93−100.

(45) Gaide, T.; Behr, A.; Arns, A.; Benski, F.; Vorholt, A. J. Hydroesterification of Methyl 10-Undecenoate in Thermomorphic Multicomponent Solvent Systems-Process Development for the Synthesis of Sustainable Polymer Precursors. *Chem. Eng. Process.* **2016**, *99*, 197−204.

(46) Buszek, K. R.; Brown, N. Improved Method for the Diimide Reduction of Multiple Bonds on Solid-Supported Substrates. *J. Org. Chem.* **2007**, *72* (8), 3125−3128.

https://doi.org/10.1021/acs.macromol.4c02074
Macromolecules XXXX, XXX, XXX−XXX

(47) Li, Z.-L.; Li, L.; Deng, X.-X.; Lv, A.; Wang, C.-H.; Du, F.-S.; Li, Z.-C. Ethylene−Ethyl Acrylate Copolymers via ADMET Polymerization: Effect of Sequence Distribution on Thermal Properties. *J. Polym. Sci., Part A: Polym. Chem.* **2013**, *51* (13), 2900−2909.
(48) McNeill, I. C.; Mohammed, M. H. A Comparison of the Thermal Degradation Behaviour of Ethylene-Ethyl Acrylate Copolymer, Low Density Polyethylene and Poly(Ethyl Acrylate). *Polym. Degrad. Stab.* **1995**, *48* (1), 175−187.
(49) Bunn, C. W.; Alcock, T. C. The Texture of Polythene. *Trans. Faraday Soc.* **1945**, *41*, 317.
(50) Crist, B. Thermodynamics of Statistical Copolymer Melting. *Polymer* **2003**, *44* (16), 4563−4572.
(51) Lehman, S. E.; Wagener, K. B.; Baugh, L. S.; Rucker, S. P.; Schulz, D. N.; Varma-Nair, M.; Berluche, E. Linear Copolymers of Ethylene and Polar Vinyl Monomers via Olefin Metathesis−Hydrogenation: Synthesis, Characterization, and Comparison to Branched Analogues. *Macromolecules* **2007**, *40* (8), 2643−2656.
(52) Patterson, A. L. The Scherrer Formula for X-Ray Particle Size Determination. *Phys. Rev.* **1939**, *56* (10), 978−982.
(53) Becker, P.; Busch, M. Modeling of Ethylene Copolymerizations with Acrylate Monomers. *Macromol. Theory Simul.* **1998**, *7* (4), 435−446.
(54) Watson, M. D.; Wagener, K. B. Ethylene/Vinyl Acetate Copolymers via Acyclic Diene Metathesis Polymerization. Examining the Effect of "Long" Precise Ethylene Run Lengths. *Macromolecules* **2000**, *33* (15), 5411−5417.
(55) Sanchez, I. C.; Eby, R. K. Thermodynamics and Crystallization of Random Copolymers. *Macromolecules* **1975**, *8* (5), 638−641.
(56) Virág, Á. D.; Juhász, Z.; Kossa, A.; Molnár, K. Combining Oscillatory Shear Rheometry and Dynamic Mechanical Analysis to Obtain Wide-Frequency Master Curves. *Polymer* **2024**, *295*, 126742.
(57) Bowden, P. B. The Elastic Modulus of an Amorphous Glassy Polymer. *Polymer* **1968**, *9*, 449−454.
(58) Luo, X.; Xie, S.; Liu, J.; Hu, H.; Jiang, J.; Huang, W.; Gao, H.; Zhou, D.; Lü, Z.; Yan, D. The Relationship between the Degree of Branching and Glass Transition Temperature of Branched Polyethylene: Experiment and Simulation. *Polym. Chem.* **2014**, *5* (4), 1305−1312.
(59) Martín, S.; Vega, J. F.; Expósito, M. T.; Flores, A.; Martínez-Salazar, J. A Three-Phase Microstructural Model to Explain the Mechanical Relaxations of Branched Polyethylene: A DSC, WAXD and DMTA Combined Study. *Colloid Polym. Sci.* **2011**, *289* (3), 257−268.
(60) García-Franco, C. A.; Harrington, B. A.; Lohse, D. J. Effect of Short-Chain Branching on the Rheology of Polyolefins. *Macromolecules* **2006**, *39* (7), 2710−2717.
(61) Nunes, R. W.; Martin, J. R.; Johnson, J. F. Influence of Molecular Weight and Molecular Weight Distribution on Mechanical Properties of Polymers. *Polym. Eng. Sci.* **1982**, *22* (4), 205−228.
(62) Jang, Y.-J.; Nguyen, S.; Hillmyer, M. A. Chemically Recyclable Linear and Branched Polyethylenes Synthesized from Stoichiometrically Self-Balanced Telechelic Polyethylenes. *J. Am. Chem. Soc.* **2024**, *146* (7), 4771−4782.
(63) Fetters, L. J.; Lohse, D. J.; García-Franco, C. A.; Brant, P.; Richter, D. Prediction of Melt State Poly(α-Olefin) Rheological Properties: The Unsuspected Role of the Average Molecular Weight per Backbone Bond. *Macromolecules* **2002**, *35* (27), 10096−10101.
(64) Fetters, L. J.; Lohse, D. J.; Milner, S. T.; Graessley, W. W. Packing Length Influence in Linear Polymer Melts on the Entanglement, Critical, and Reptation Molecular Weights. *Macromolecules* **1999**, *32* (20), 6847−6851.
(65) Fetters, L. J.; Lohse, D. J.; Richter, D.; Witten, T. A.; Zirkel, A. Connection between Polymer Molecular Weight, Density, Chain Dimensions, and Melt Viscoelastic Properties. *Macromolecules* **1994**, *27* (17), 4639−4647.
(66) Hoy, R. S.; Kröger, M. Unified Analytic Expressions for the Entanglement Length, Tube Diameter, and Plateau Modulus of Polymer Melts. *Phys. Rev. Lett.* **2020**, *124* (14), 147801.
(67) Bensason, S.; Nazarenko, S.; Chum, S.; Hiltner, A.; Baer, E. Elastomeric Blends of Homogeneous Ethylene-Octene Copolymers. *Polymer* **1997**, *38* (15), 3913−3919.
(68) Koo, C. M.; Hillmyer, M. A.; Bates, F. S. Structure and Properties of Semicrystalline−Rubbery Multiblock Copolymers. *Macromolecules* **2006**, *39* (2), 667−677.
(69) Maynard, L. A.; DeButts, B. L.; Barone, J. R. Mechanical and Thermal Properties of Polyolefin Thermoplastic Elastomer Blends. *Plast., Rubber Compos.* **2019**, *48* (8), 338−346.
(70) Adhikari, R.; Godehardt, R.; Lebek, W.; Frangov, S.; Michler, G. H.; Radusch, H.-J.; Calleja, F. J. B. Morphology and Micromechanical Properties of Ethylene/1-octene Copolymers and Their Blends with High Density Polyethylene. *Polym. Adv. Technol.* **2005**, *16* (2−3), 156−166.
(71) Sang, R.; Kucmierczyk, P.; Dühren, R.; Razzaq, R.; Dong, K.; Liu, J.; Franke, R.; Jackstell, R.; Beller, M. Synthesis of Carboxylic Acids by Palladium-Catalyzed Hydroxycarbonylation. *Angew. Chem. Int. Ed.* **2019**, *58* (40), 14365−14373.

https://doi.org/10.1021/acs.macromol.4c02074
Macromolecules XXXX, XXX, XXX−XXX